

AD-A252 364



2

AD

TECHNICAL REPORT ARCCB-TR-92018

SOLVING THE EULER EQUATIONS USING ADAPTIVE MESH MOTION AND REFINEMENT

DAVID C. ARNEY
RUPAK BISWAS
JOSEPH E. FLAHERTY

S DTIC
ELECTE
JUL 07 1992 **D**
A

APRIL 1992



**US ARMY ARMAMENT RESEARCH,
DEVELOPMENT AND ENGINEERING CENTER
CLOSE COMBAT ARMAMENTS CENTER
BENÉT LABORATORIES
WATERVLIET, N.Y. 12189-4050**



APPROVED FOR PUBLIC RELEASE; DISTRIBUTION UNLIMITED

92-17628



DISCLAIMER

The findings in this report are not to be construed as an official Department of the Army position unless so designated by other authorized documents.

The use of trade name(s) and/or manufacturer(s) does not constitute an official indorsement or approval.

DESTRUCTION NOTICE

For classified documents, follow the procedures in DoD 5200.22-M, Industrial Security Manual, Section II-19 or DoD 5200.1-R, Information Security Program Regulation, Chapter IX.

For unclassified, limited documents, destroy by any method that will prevent disclosure of contents or reconstruction of the document.

For unclassified, unlimited documents, destroy when the report is no longer needed. Do not return it to the originator.

REPORT DOCUMENTATION PAGE

Form Approved
OMB No. 0704-0188

Public reporting burden for this collection of information is estimated to average 1 hour per response, including the time for reviewing instructions, searching existing data sources, gathering and maintaining the data needed, and completing and reviewing the collection of information. Send comments regarding this burden estimate or any other aspect of this collection of information, including suggestions for reducing this burden, to Washington Headquarters Services, Directorate for Information Operations and Reports, 1215 Jefferson Davis Highway, Suite 1204, Arlington, VA 22202-4302, and to the Office of Management and Budget, Paperwork Reduction Project (0704-0188), Washington, DC 20503.

1. AGENCY USE ONLY (Leave blank)	2. REPORT DATE April 1992	3. REPORT TYPE AND DATES COVERED Final	
4. TITLE AND SUBTITLE SOLVING THE EULER EQUATIONS USING ADAPTIVE MESH MOTION AND REFINEMENT		5. FUNDING NUMBERS AMCMS: 6111.02.H610.0 PRON: 1A94Z9CANMSC	
6. AUTHOR(S) David C. Arney (USMA, West Point, NY), Rupak Biswas (RPI, Troy, NY), and Joseph E. Flaherty (RPI and Benet)		8. PERFORMING ORGANIZATION REPORT NUMBER ARCCB-TR-92018	
7. PERFORMING ORGANIZATION NAME(S) AND ADDRESS(ES) U.S. Army ARDEC Benet Laboratories, SMCAR-CCB-TL Watervliet, NY 12189-4050		10. SPONSORING / MONITORING AGENCY REPORT NUMBER	
9. SPONSORING / MONITORING AGENCY NAME(S) AND ADDRESS(ES) U.S. Army ARDEC Close Combat Armaments Center Picatinny Arsenal, NJ 07806-5000		10. SPONSORING / MONITORING AGENCY REPORT NUMBER	
11. SUPPLEMENTARY NOTES Presented at the Seventh Army Conference on Applied Mathematics and Computing, U.S. Military Academy, West Point, NY, 6-9 June 1989. Published in Proceedings of the Conference.			
12a. DISTRIBUTION / AVAILABILITY STATEMENT Approved for public release; distribution unlimited.		12b. DISTRIBUTION CODE	
13. ABSTRACT (Maximum 200 words) We use an adaptive mesh moving and refinement finite volume method to solve the transient Euler equations of compressible flow in one and two space dimensions. Numerical solutions are generated by a MacCormack scheme with Davis's artificial viscosity model. Richardson's extrapolation is used to calculate estimates of the local discretization error which can be used to control mesh motion and refinement. Questions regarding the optimal combination of adaptive strategies and the characterization of the initial mesh are investigated. Results indicate that local mesh refinement with and without mesh moving provide dramatic improvements in accuracy over uniform mesh solutions; that mesh motion provides good results on relatively fine initial meshes; that each problem has an optimal initial mesh and that it is more efficient to begin with a coarser than optimal mesh and refine rather than starting with too fine a mesh; and that a combination of both the adaptive strategies produced the most accurate solutions.			
14. SUBJECT TERMS Adaptive Systems, Euler Equations, Local Mesh Refinement, Mesh Motion, Partial Differential Equations, Refinement		15. NUMBER OF PAGES 18	16. PRICE CODE
17. SECURITY CLASSIFICATION OF REPORT UNCLASSIFIED	18. SECURITY CLASSIFICATION OF THIS PAGE UNCLASSIFIED	19. SECURITY CLASSIFICATION OF ABSTRACT UNCLASSIFIED	20. LIMITATION OF ABSTRACT UL

TABLE OF CONTENTS

	<u>Page</u>
ABSTRACT	1
INTRODUCTION	2
NUMERICAL EXPERIMENTS	3
CONCLUSIONS	8
REFERENCES	16

TABLES

1. NORMALIZED CPU TIME, NUMBER OF SPACE-TIME CELLS, AND EFFORT PER UNIT ACCURACY AT $t = 0.35$ WITH DIFFERENT INITIAL BASE MESHES FOR EXAMPLE 1	5
2. NORMALIZED CPU TIME, NUMBER OF SPACE-TIME CELLS, AND GLOBAL L_1 ERROR AT $t = 0.35$ AS A FUNCTION OF THE LOCAL ERROR TOLERANCE FOR EXAMPLE 1 USING LOCAL MESH REFINEMENT	5
3. NORMALIZED CPU TIME, NUMBER OF SPACE-TIME CELLS, AND GLOBAL L_1 ERROR AT $t = 0.35$ FOR ADAPTIVE AND STANDARD SOLUTIONS OF EXAMPLE 1	7

LIST OF ILLUSTRATIONS

1. Effort per unit accuracy vs. number of elements in the base mesh for Example 1	6
2. Solutions, mesh trajectories, and time step profile for computations performed with a stationary uniform mesh of 16 cells for Example 1	9
3. Solutions, mesh trajectories, and time step profile for computations performed with adaptive mesh motion on a mesh of 16 cells for Example 1	10
4. Solutions, mesh trajectories, and time step profile for computations performed with adaptive local mesh refinement for Example 1	11

5. Solutions, mesh trajectories, and time step profile for computations performed with both adaptive mesh motion and local mesh refinement for Example 1 12

6. Solutions, mesh trajectories, and time step profile for computations performed with adaptive mesh motion on a mesh of 50 cells for Example 1 13

7. Density contours for Example 2 at $t = 0.0096$ obtained from the exact solution (upper left) and by computed solutions on a uniform stationary mesh (upper right), a uniform stationary base mesh with one level of refinement (lower left), and a moving base mesh with one level of refinement (lower right) 14

8. Spatial meshes at $t = 0.0096$ for Example 2 using one level of local mesh refinement on a uniform stationary base mesh (left) and a moving base mesh (right) 15

SOLVING THE EULER EQUATIONS USING ADAPTIVE MESH MOTION AND REFINEMENT¹

David C. Arney

Department of Mathematics
United States Military Academy
West Point, NY 10996-1786

Rupak Biswas

Department of Computer Science
Rensselaer Polytechnic Institute
Troy, NY 12180-3590

Joseph E. Flaherty

Department of Computer Science
Rensselaer Polytechnic Institute
Troy, NY 12180-3590

and

U.S. Army Armament, Munition, and Chemical Command
Armament Research and Development Center
Close Combat Armaments Center
Benét Laboratory
Watervliet, NY 12189-4050

Accession For	
NTIS CRA&I	<input checked="" type="checkbox"/>
DTIC TAB	<input type="checkbox"/>
Unannounced	<input type="checkbox"/>
Justification	
By	
Distribution/	
Availability Code	
Dist	Availability for Special
A-1	



ABSTRACT. We use an adaptive mesh moving and refinement finite volume method to solve the transient Euler equations of compressible flow in one and two space dimensions. Numerical solutions are generated by a MacCormack scheme with Davis's artificial viscosity model. Richardson's extrapolation is used to calculate estimates of the local discretization error which can be used to control mesh motion and refinement. Questions regarding the optimal combination of adaptive strategies and the characterization of the initial mesh are investigated. Results indicate that local mesh refinement with and without mesh moving provide dramatic improvements in accuracy over uniform mesh solutions; that mesh motion provides good results on relatively fine initial meshes; that each problem has an optimal initial mesh and that it is more efficient to begin with a coarser than optimal mesh and refine rather than starting with too fine a mesh; and that a combination of both the adaptive strategies produced the most accurate solutions.

¹ This research was partially supported by the SDIO/IST under management of the U. S. Army Research Office under Contract Number DAAL 03-86-K-0112.

1. INTRODUCTION. Our goal is to develop reliable, robust, and efficient software for solving hyperbolic partial differential equations. With this in mind, Arney and Flaherty [4] developed an adaptive procedure combining mesh motion and mesh refinement for solving one- and two-dimensional vector systems of time-dependent partial differential equations. The solution, mesh motion, and local refinement procedures were explicit and independent of each other; thus, modules can easily be replaced.

Arney and Flaherty's [4] method solves vector systems of hyperbolic conservation laws having the form

$$\mathbf{u}_t + \mathbf{f}_x(x, y, t, \mathbf{u}) + \mathbf{g}_y(x, y, t, \mathbf{u}) = 0, \quad (1a)$$

with initial conditions

$$\mathbf{u}(x, y, 0) = \mathbf{u}_0(x, y), \quad (1b)$$

and with appropriate well-posed boundary conditions on a one- or two-dimensional domain Ω . Their adaptive approach consists of moving a coarse "base" mesh of quadrilateral cells to follow fronts and reduce dispersive errors. Recursive refinement of mesh cells is performed when necessary to satisfy a prescribed local error tolerance. Solutions are generated using MacCormack's [10] finite volume scheme coupled with Davis's [8] artificial viscosity model to make the scheme total variation diminishing (TVD). Local motion and refinement indicators on each cell of the mesh are used to control mesh motion and refinement, respectively. They used an estimate of the local discretization error obtained by Richardson's extrapolation [2,11] as the mesh refinement indicator. For the examples presented in this paper, we used a normalized solution gradient as the mesh movement indicator, although other choices are possible as long as the indicator is large where additional resolution is required and small where less resolution is desired. An automatic time step adjustment feature, based on maximizing the Courant stability condition, is also provided in our algorithm.

The generation of a proper initial mesh is important for the efficiency of any adaptive algorithm. Initially we create a uniform mesh on Ω having a specified number of nodes without considering the possibility of any high-error regions. A global mesh refinement is performed on the first time step to estimate the discretization error of the initial data. The nodes of the mesh are then placed to equidistribute this error estimate. As time evolves, these nodes are dynamically moved to reduce dispersive errors.

Arney and Flaherty [4,5] perform mesh motion based on an intuitive approach by identifying computational cells having large motion indicators and clustering them into isolated regions that are presumed to contain similar solution characteristics. The center of motion indicators of each clustered region is moved so as to follow the dynamics of the solution. Remaining portions of the mesh are moved according to an algebraic function so as to produce a smooth grid having minimal distortion. Most mesh points cannot move independently but must be coupled to their immediate neighbors. The amount of movement is determined by a function which ensures that the center $r_m(t)$ of error clusters moves according to the differential equation

$$\ddot{r}_m + \lambda \dot{r}_m = 0, \quad (2)$$

used by Coyle et al. [7]. Clustered regions created at one time step can subsequently be destroyed when a dynamic phenomenon subsides. Similarly, two or more clusters can be united when structures of the solution intersect.

Results obtained by using Arney and Flaherty's [1,3,4,5] adaptive algorithm in one and two dimensions indicated that, in some instances, proper mesh motion was capable of dramatically reducing errors for a modest increase in the cost of computation. In general, however, mesh motion alone cannot produce solutions that satisfy arbitrarily prescribed accuracy requirements. They, therefore, combined mesh motion with a local temporal and spatial cellular mesh refinement strategy [4,6]. The space-time cells of a mesh that violated the prescribed error tolerance were gathered into clusters and were recursively bisected in space and time. The problem was solved locally on the successively smaller domains created by the clustering and refinement. Initial and boundary data for any refined mesh were determined by interpolation from their "parent" coarser mesh. Error tolerances involved control of the local error per unit time step and were, thus, halved at each refinement to account for the binary temporal refinement.

A dynamic tree structure, where fine grids are regarded as offspring of coarser ones, is used to manage the data associated with the motion and refinement strategies. Solutions were generated by a preorder traversal of the tree; thus, solutions on all fine meshes preceded those on coarser ones.

Our results on solving shock problems for the one- and two-dimensional Euler equations are presented in Section 2. We explore the relationship of the base mesh to the level of refinement. We found, for example, that it is more effective to begin with a coarse mesh and perform more refinement than to create a finer mesh which needs less refinement. Effective mesh motion, on the other hand, required a finer base mesh rather than a coarser one. The combination of mesh motion and refinement produced the best results. Local refinement with and without mesh moving provide substantial improvements in accuracy per unit cost relative to computations on uniform stationary mesh solutions.

2. NUMERICAL EXPERIMENTS. Computer codes for one- and two-dimensional problems based on Arney and Flaherty's [4] algorithm have been implemented in FORTRAN on an IBM 3090-200S computer and tested on several problems [1,4]. In this paper, we consider examples involving solutions of the Euler equations for a one-dimensional shock tube and a two-dimensional piston problem. The Euler equations for a perfect compressible fluid are studied in their conservative form

$$\mathbf{u}_t + \mathbf{f}_x(\mathbf{u}) + \mathbf{g}_y(\mathbf{u}) = 0, \quad (3a)$$

where

$$\mathbf{u} = \begin{bmatrix} \rho \\ \rho u \\ \rho v \\ e \end{bmatrix}, \quad \mathbf{f}(\mathbf{u}) = \begin{bmatrix} \rho u \\ \rho u^2 + p \\ \rho uv \\ u(e + p) \end{bmatrix}, \quad \mathbf{g}(\mathbf{u}) = \begin{bmatrix} \rho v \\ \rho vu \\ \rho v^2 + p \\ v(e + p) \end{bmatrix}. \quad (3b,c,d)$$

Here, ρ is the fluid density; u and v are the Cartesian components of the velocity vector; e is the total internal energy per unit volume; and the subscripts x , y , and t denote partial differentiation with respect to the spatial coordinates and time, respectively. The pressure p is evaluated according to the ideal gas equation of state as

$$p = (\gamma - 1)[e - \rho(u^2 + v^2)/2], \quad (4)$$

where γ is the specific heat ratio of the fluid. Computational experiments were conducted with $\gamma = 1.4$. Solution accuracy is appraised in the L_1 norm

$$\|e(\cdot, \cdot, t)\|_1 = \max_{1 \leq j \leq 4} \int_{\Omega} |e_j(x, y, t)| dx dy, \quad (5)$$

where $e_j(x, y, t)$ is a piecewise constant approximation of $u_j(x, y, t) - U_j$ obtained by using values at cell centers.

Example 1. Consider Sod's [12] one-dimensional shock tube problem which consists of solving (3,4) with $v = 0$ and $\partial(\cdot)/\partial y = 0$ subject to the initial conditions

$$\begin{bmatrix} \rho(x, 0) \\ p(x, 0) \\ u(x, 0) \end{bmatrix} = \begin{cases} [1.0, 1.0, 0.0]^T, & \text{if } -0.2 \leq x \leq 0.5 \\ [0.125, 0.1, 0.0]^T, & \text{if } 0.5 < x \leq 1.5 \end{cases} \quad (6)$$

A diaphragm at $x = 0.5$ separates two regions of a tube that contain gases at different densities and pressures. The two regions are in a constant state and both fluids are initially at rest. At time $t = 0$ the diaphragm is ruptured and three waves are generated: a shock moving with velocity 1.7522, a contact discontinuity moving with velocity 0.9275, and an expansion wave centered between $0.5 - 1.1832t \leq x \leq 0.5 - 0.0703t$. The exact solution [13] of this problem is

$$\begin{bmatrix} u(x, t) \\ \rho(x, t) \\ p(x, t) \end{bmatrix} = \begin{cases} [0.0, 1.0, 1.0]^T, & \text{if } \eta \leq -1.1832 \\ [0.9860 + \eta/1.2, (1 - u/5.9161)^5, \rho^{1.4}]^T, & \text{if } -1.1832 \leq \eta \leq -0.0703 \\ [0.9275, 0.4263, 0.3031]^T, & \text{if } -0.0703 \leq \eta < 0.9275 \\ [0.9275, 0.2656, 0.3031]^T, & \text{if } 0.9275 < \eta < 1.7522 \\ [0.0, 0.125, 0.1]^T, & \text{if } 1.7522 < \eta \end{cases} \quad (7)$$

where $\eta = (x - 0.5)/t$.

The "base" mesh is the coarsest mesh used to solve a problem. It reflects the scale on which dominant temporal and spatial changes in the solution occur. Selecting too coarse a base mesh will result in excessive refinement. Selecting too fine a base mesh will be inefficient. At present, selection of the base mesh is at the discretion of the user and in this first experiment we hope to provide guidance for this choice as well as for future automated base mesh selection procedures. Six cases having base meshes of $N = 2^k$, $k = 3, 4, \dots, 8$, cells were solved on $0 < t \leq 0.35$. The maximum number of refinement levels, the initial time step, and the local discretization error were set at $8-k$, $3 \times 2^{9-k} \times 10^{-4}$, and $2^{5-k} \times 10^{-5}$, $k = 3, 4, \dots, 8$, respectively, so that the finest allowable discretization and local error tolerance were constant for all six cases.

N	Error Tolerance ($\times 10^5$)	Max. No. Refinement Levels	Normalized CPU Time (Effort)	No. Space-Time Cells	Effort per Unit Accuracy ($\times 10^3$)
8	4.0	5	1.295	28162	3.71
16	2.0	4	1.066	23026	2.17
32	1.0	3	1.000	21006	2.24
64	0.5	2	1.104	21396	2.67
128	0.25	1	1.533	25996	3.89
256	0.125	0	4.104	63744	6.70

Table 1. Normalized CPU time, number of space-time cells, and effort per unit accuracy at $t = 0.35$ with different initial base meshes for Example 1. The parameters are adjusted so that the finest discretization and the corresponding local error tolerance are constant for all cases.

Results for the normalized CPU time, the number of space-time cells, and the effort per unit accuracy are reported in Table 1 for each of the six cases. Effort per unit accuracy is the product of the normalized CPU time and the L_1 error at terminal time (0.35 in this case). In Figure 1, we show how the effort per unit accuracy varies with the logarithm of the number of cells in the base mesh. It is preferable to select a coarser base mesh than a finer one since, with our procedures, refinement of a coarse mesh will decrease the effort/accuracy ratio. The number of space-time cells vary in approximately the same ratio as the CPU time suggesting that the overhead associated with data management is minimal.

Error Tolerance ($\times 10^5$)	Normalized CPU Time	No. of Space-Time Cells	$\ e\ _1 (\times 10^3)$
128.0	1.000	910	25.7
32.0	4.473	7532	12.7
8.0	9.370	19322	6.20
2.0	15.610	34562	3.03

Table 2. Normalized CPU time, number of space-time cells, and global L_1 error at $t = 0.35$ as a function of the local error tolerance for Example 1 using local mesh refinement.

We continued our experiments by solving this problem on $-0.2 \leq x \leq 1.5$ for $0 < t \leq 0.35$ using local mesh refinement on 16-element base meshes, an initial time step

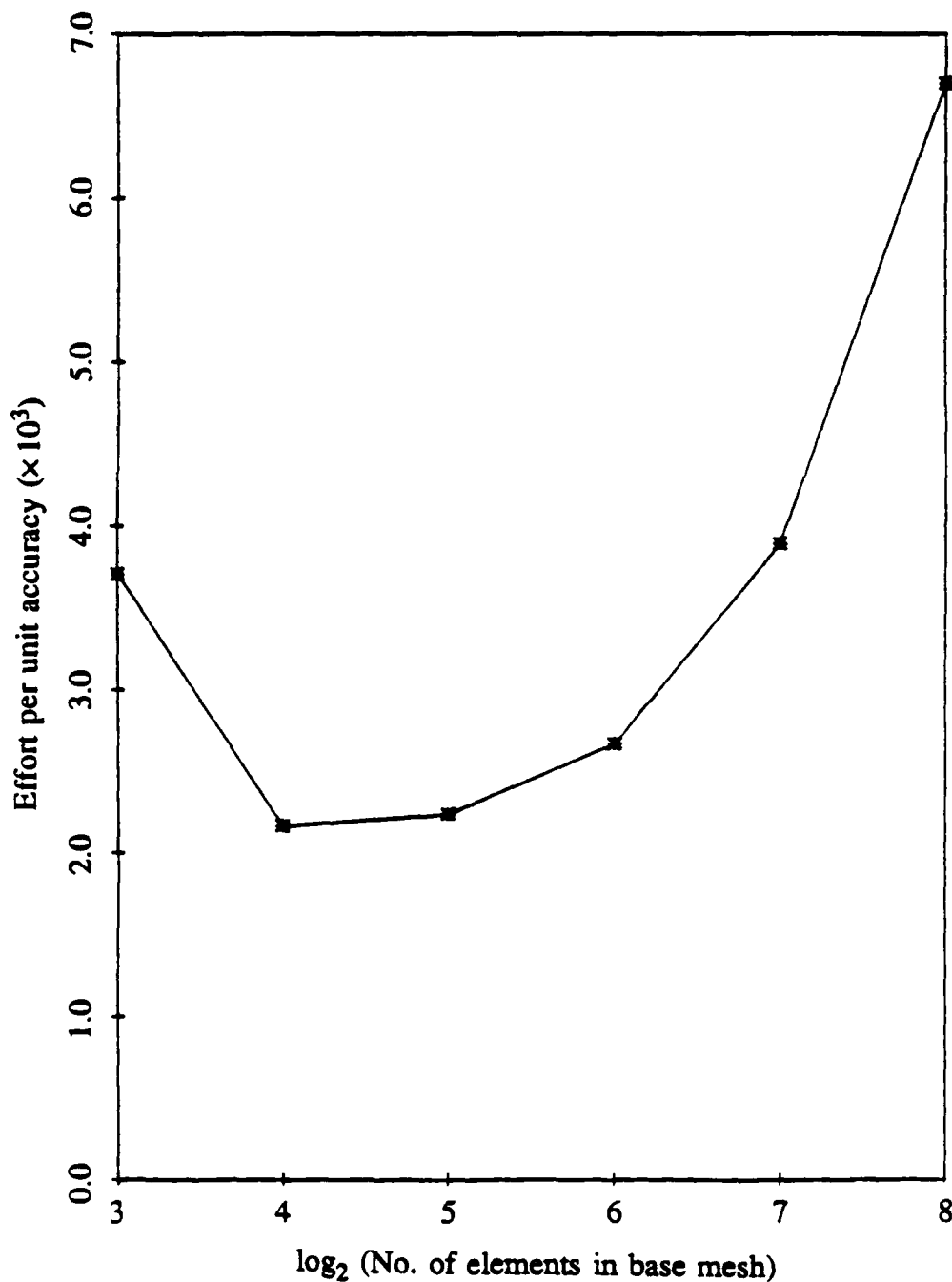


Figure 1. Effort per unit accuracy vs. number of elements in the base mesh for Example 1.

of 0.0035, and with varying error tolerances. Refinement was restricted to a maximum of four levels to avoid excessive refinement near shocks. The normalized CPU time, the number of space-time cells used to solve the problem, and the errors in L_1 at $t = 0.35$ are presented in Table 2 as functions of the local discretization error tolerance. For small tolerances, the CPU times and the number of space-time cells increase at approximately

the same rate as the L_1 error decreases, again indicating a minimal overhead associated with refinement. The decrease in the local pointwise error tolerance is quadratic when compared with the actual global L_1 error, which is what one would expect for problems having smooth solutions. The result apparently carries over to this shock problem.

Strategy	Normalized CPU Time	No. of Space-Time Cells	$\ e\ _1 (\times 10^3)$
Uniform Mesh	1.000	576	30.7
Coarse Mesh Motion	2.026	1152	16.9
Refinement	19.009	34562	3.03
Motion & Refinement	26.532	44602	1.88
Fine Mesh Motion	8.584	12690	4.37

Table 3. Normalized CPU time, number of space-time cells, and global L_1 error at $t = 0.35$ for adaptive and standard solutions of Example 1.

The third experiment involves comparing adaptive solutions obtained using mesh motion, local mesh refinement, and mesh motion plus local refinement with one obtained on a uniform mesh. In each case, a 16-element base mesh and an initial time step of 0.0035 was selected. An error tolerance of 0.00002 was used for those solutions that involved refinement. A fifth solution involving motion of a finer 50-element mesh was also generated. Data similar to that presented in Table 2 is displayed in Table 3 comparing the results of different adaptive strategies with those on a stationary uniform mesh. In Figures 2 to 6 we display the calculated density as a function of x at $t = 0, 0.09, 0.18, 0.27,$ and $0.35,$ the meshes used, and the time steps selected for each of the solutions shown in Table 3. The uniform mesh solution shown in Figure 2 exhibits excessive diffusion at the shock, at the contact surface, and in the expansion region. However, the time step increases rapidly in accordance with the Courant condition. A larger initial time step could clearly have been used; however, we wanted to use the same initial time step for all the cases. In Figure 3 we show that the moving mesh procedure follows the dominant features of the solution. Results are clearly superior to those in Figure 2, but the mesh is too coarse to obtain good resolution everywhere. The results in Figure 6 demonstrate that far better resolution is obtained when a finer mesh consisting of 50 elements is used; however, this mesh did not move correctly in the expansion region because the mesh movement indicator is too small there. The initial mesh generator distributes a specified number of nodes N based on the initial data. In this case, the initial data has a jump discontinuity at $x = 0.5,$ so nodes were clustered around that point and then gradually spread across the domain. There are too many nodes in the expansion region in relation to the small magnitude of the movement indicator to produce adequate motion there. A static rezone of the mesh could alleviate this problem. The time steps of both solutions with mesh moving (Figures 3 and 6) are erratic for small times while the mesh is

adjusting itself to the three breaking waves. Time steps increase at the same rate as those for the uniform mesh solution of Figure 2 when a coarser mesh is used. Incorrect motion of the fine mesh in the expansion region (Figure 6) prevented a similar increase of the time step. The results depicted in Figure 4 show that refinement was correctly performed at all critical points of the calculation. In each case, shocks are captured sharply with the correct speed. As expected with Davis's [8] artificial viscosity model, diffusive effects are more pronounced near the contact surface than at the shock. Results obtained using both mesh motion and refinement are depicted in Figure 5. The results have improved somewhat but at the cost of a significantly higher computational effort relative to the solution of Figure 4. This suggests that mesh motion, with or without refinement, is not competitive with refinement alone. Additional experimentation is needed to determine a better combination of mesh moving and refinement.

Example 2. Consider the solution of the Euler equations (3,4) in a region exterior to an infinite cylindrical piston that is expanding radially creating a radially expanding shock wave. We ignore the cylindrical symmetry and solve this problem in one quadrant of the two-dimensional rectangular domain $-0.05 \leq x, y \leq 0.05$ with the two-dimensional algorithm of Arney and Flaherty [4]. Self-similar solutions of this test problem are obtained by solving a pair of ordinary differential equations (by numerical integration) for the radial velocity and acoustic speed [9].

We solved this problem for $0 < t \leq 0.0096$ with the piston initially positioned at a radius of 0.016023 and having a velocity of 1.6185. Numerical solutions were calculated on a 26×26 spatial mesh (i) without adaptation, (ii) with one level of local refinement, and (iii) with mesh motion and one level of refinement. Contours of the density at $t = 0.0096$ are presented for the exact and three numerical solutions in Figure 7. The spatial meshes produced by the two adaptive strategies at $t = 0.0096$ are shown in Figure 8.

Clearly one level of refinement is not sufficient to adequately resolve the structure of this solution. We were forced to limit our computations to this level because of memory restrictions on our computing system. Nevertheless, local refinement with and without mesh moving provide improvements in accuracy over uniform stationary mesh solutions. Detailed quantitative comparisons have yet to be performed; however, qualitatively, the expanding shock is sharper in both adaptive solutions. The combination of mesh motion and refinement provides additional improvement.

3. CONCLUSIONS. We have applied an adaptive mesh motion and refinement method for time-dependent partial differential equations to the one- and two-dimensional Euler equations. Our method can be used with several numerical methods and local error indicators to produce solutions that satisfy prescribed local tolerances. Mesh motion is global and is performed at every time step. Mesh refinement is cellular and can be used on irregular or moving meshes of quadrilateral cells.

Our results indicate that mesh refinement can be used to achieve prescribed levels of accuracy. Refinement is easy, recursive, and works well. It appears to be computationally efficient for a given accuracy level. Proper mesh movement improved the computed results. Refinement has a definite advantage over mesh motion in that it is inferred in an a posteriori manner from a preliminary solution whereas our mesh motion is applied in an

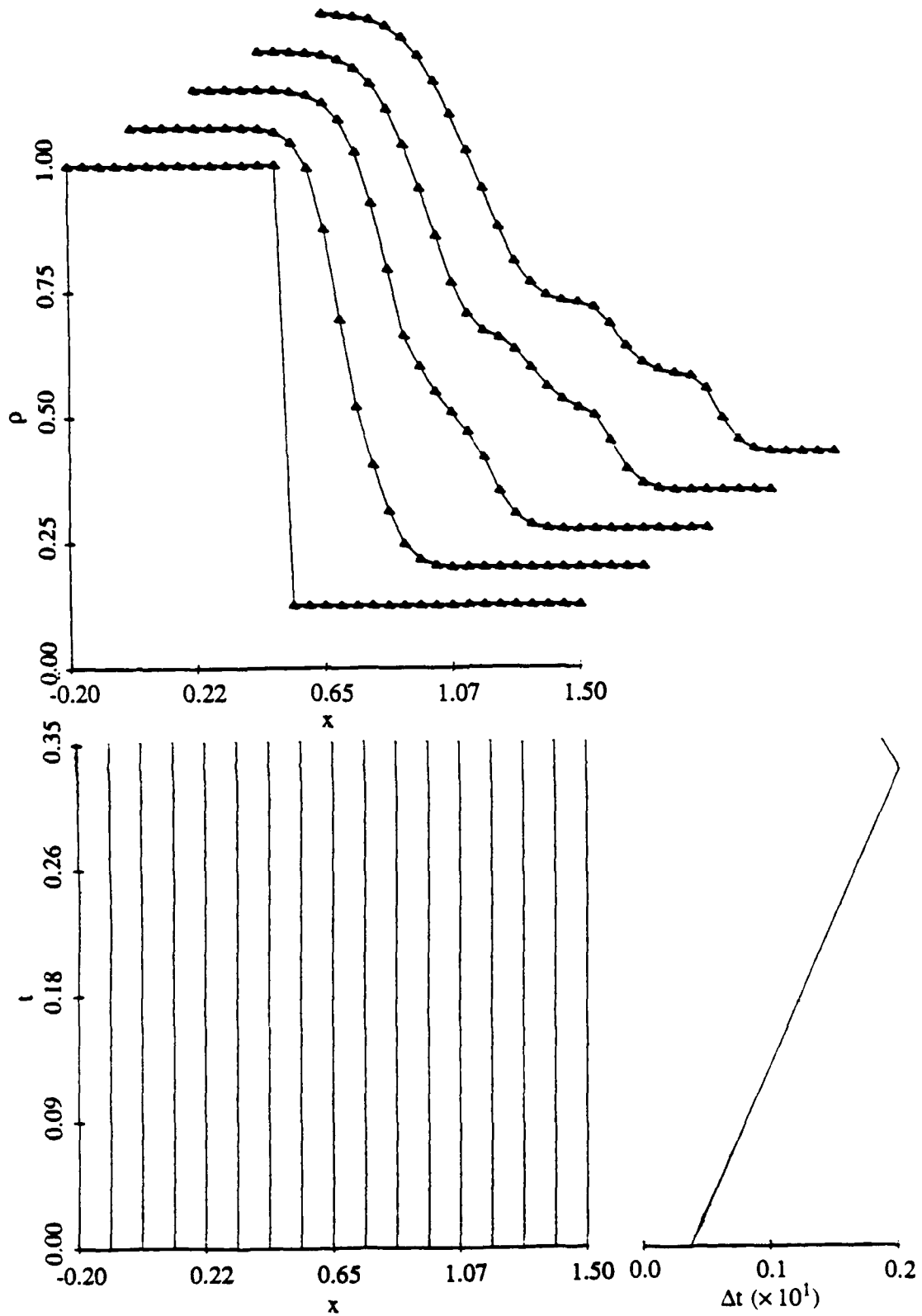


Figure 2. Solutions, mesh trajectories, and time step profile for computations performed with a stationary uniform mesh of 16 cells for Example 1.

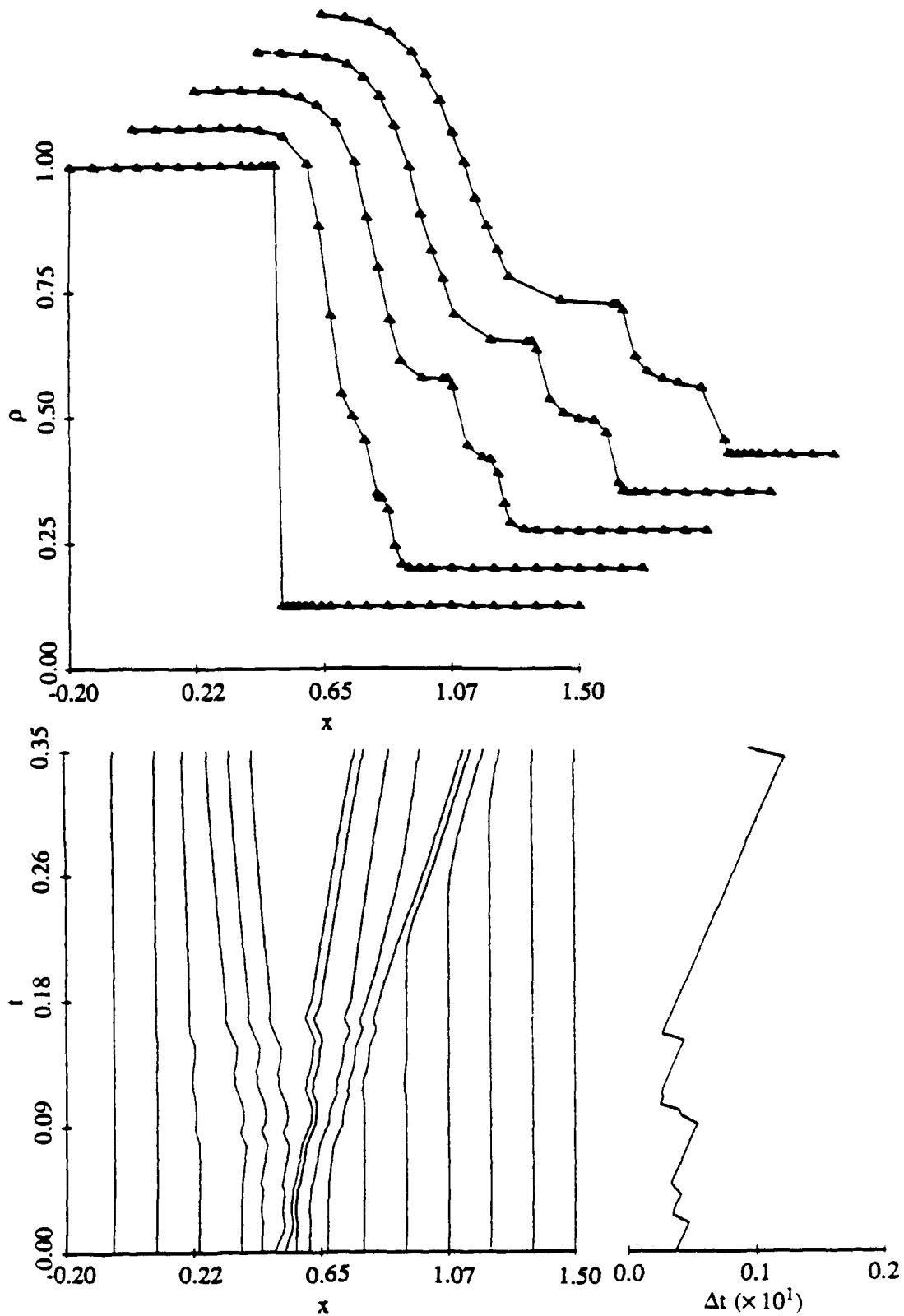


Figure 3. Solutions, mesh trajectories, and time step profile for computations performed with adaptive mesh motion on a mesh of 16 cells for Example 1.

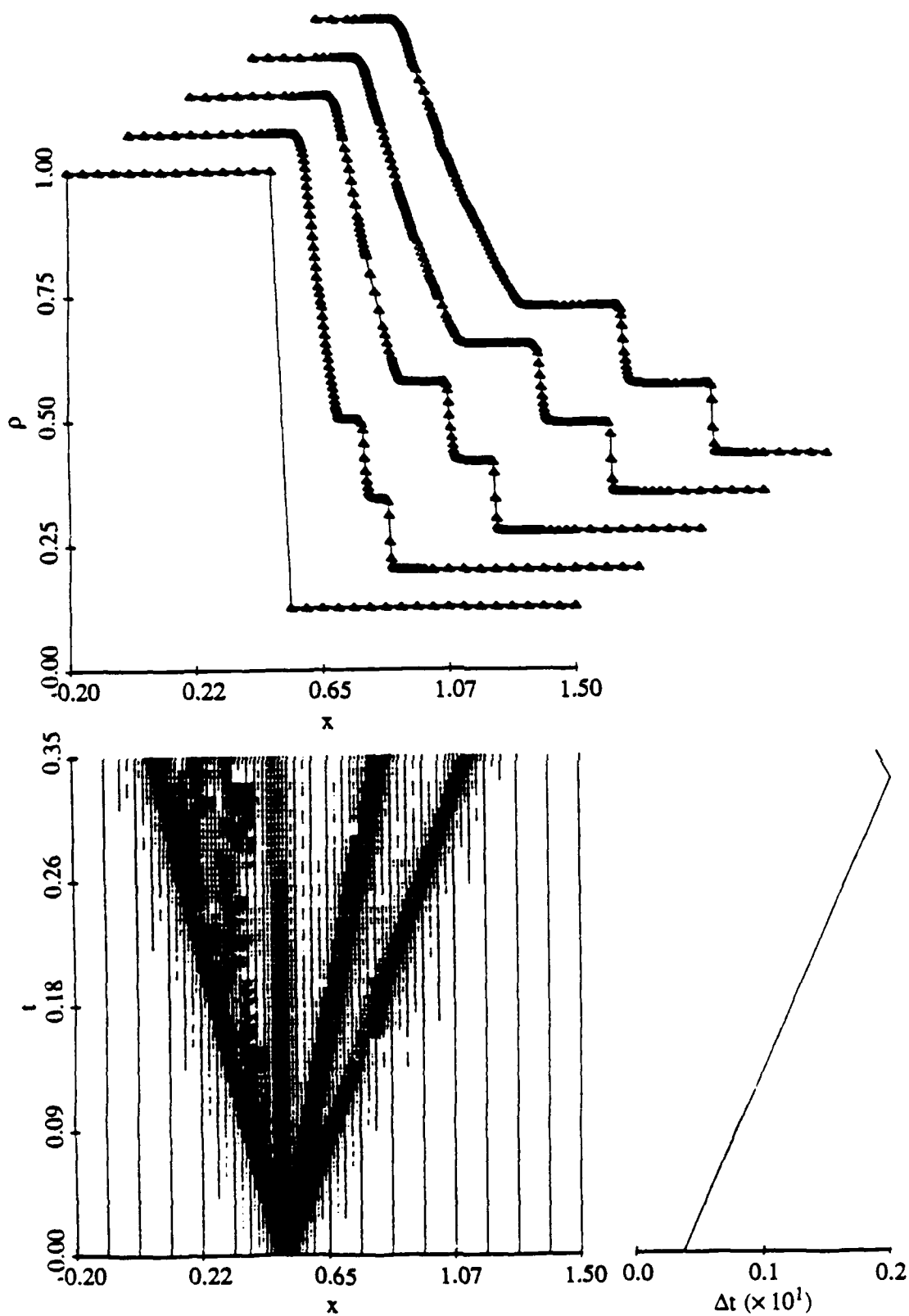


Figure 4. Solutions, mesh trajectories, and time step profile for computations performed with adaptive local mesh refinement for Example 1.

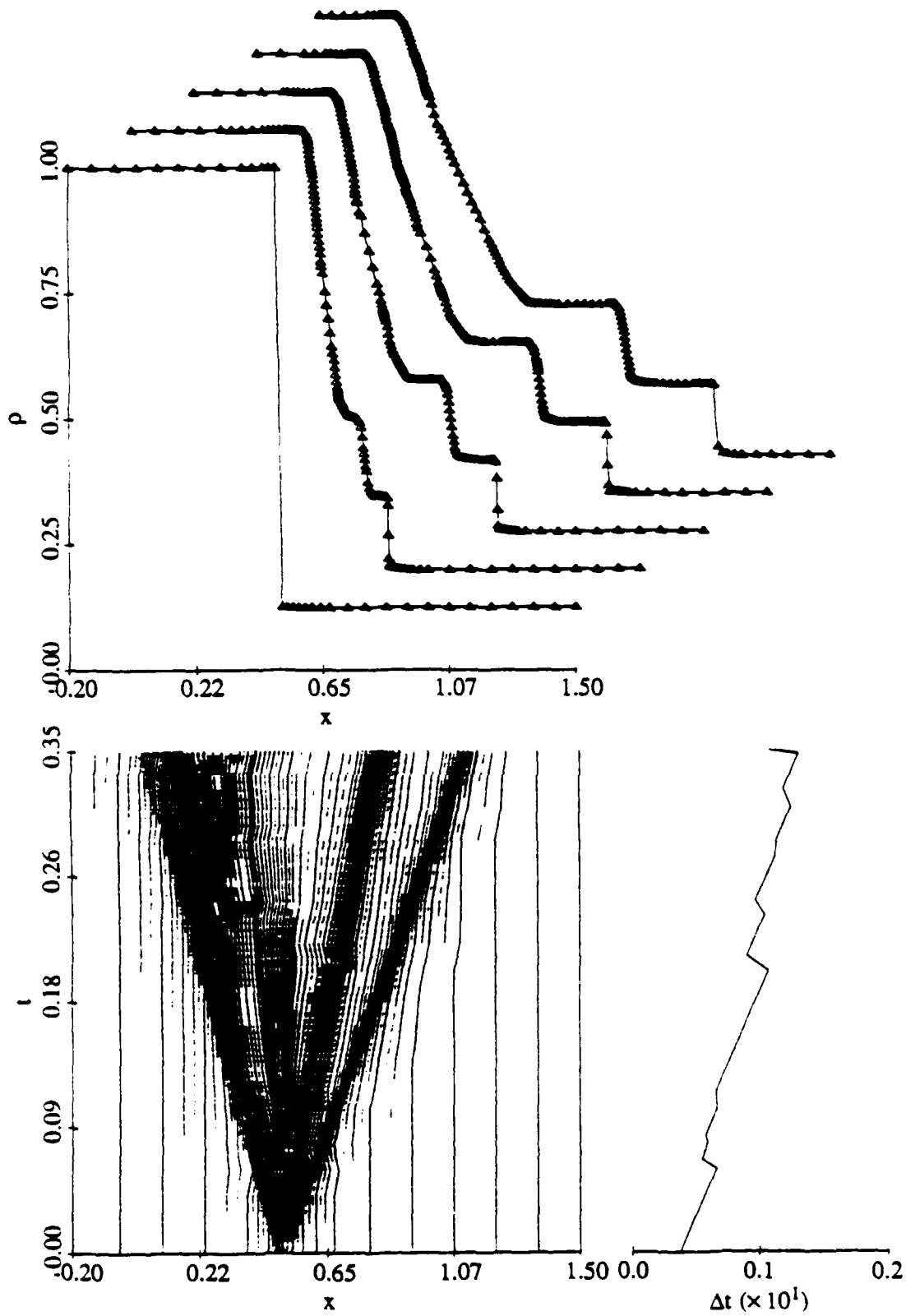


Figure 5. Solutions, mesh trajectories, and time step profile for computations performed with both adaptive mesh motion and local mesh refinement for Example 1.

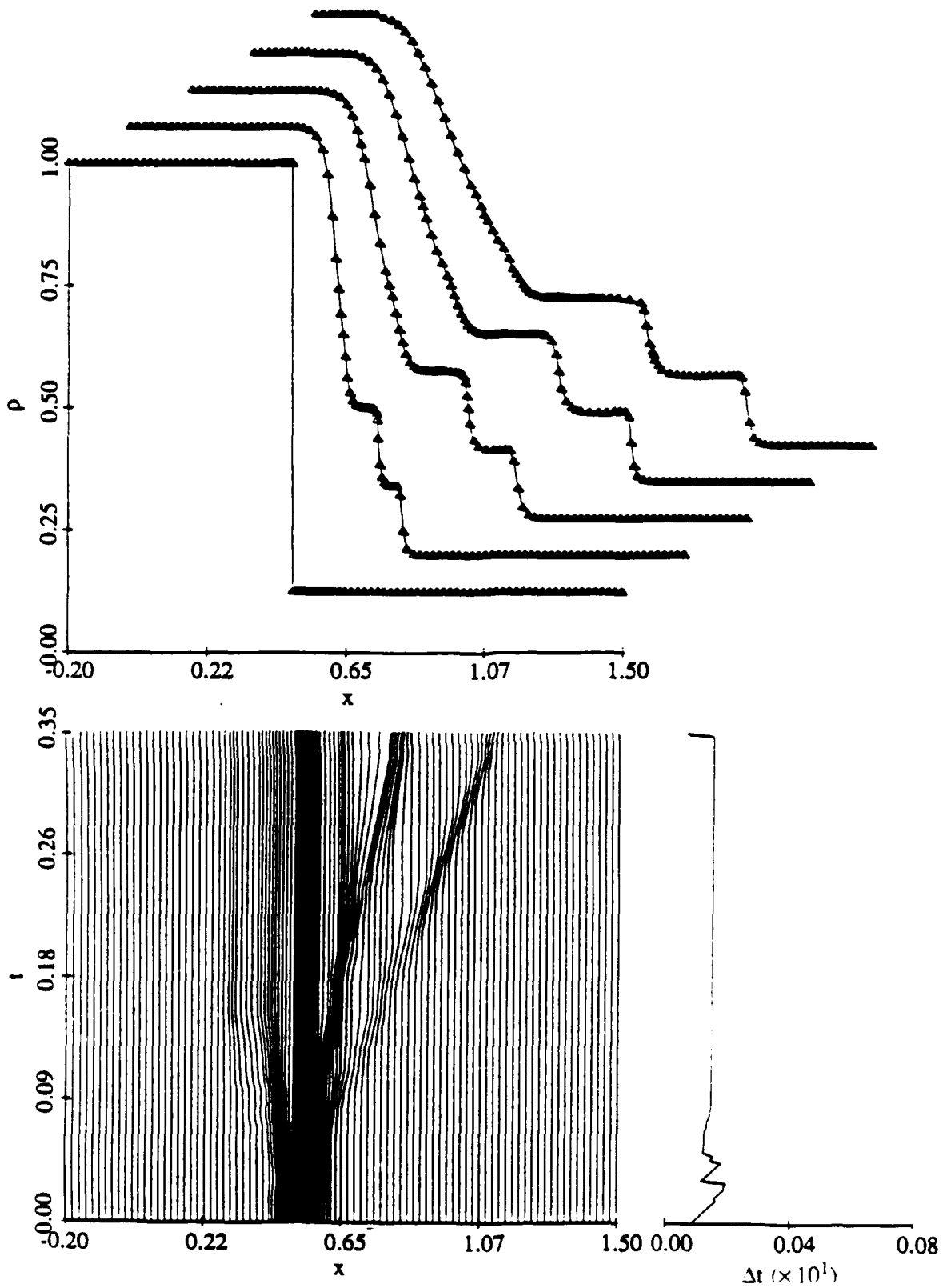


Figure 6. Solutions, mesh trajectories, and time step profile for computations performed with adaptive mesh motion on a mesh of 50 cells for Example 1.

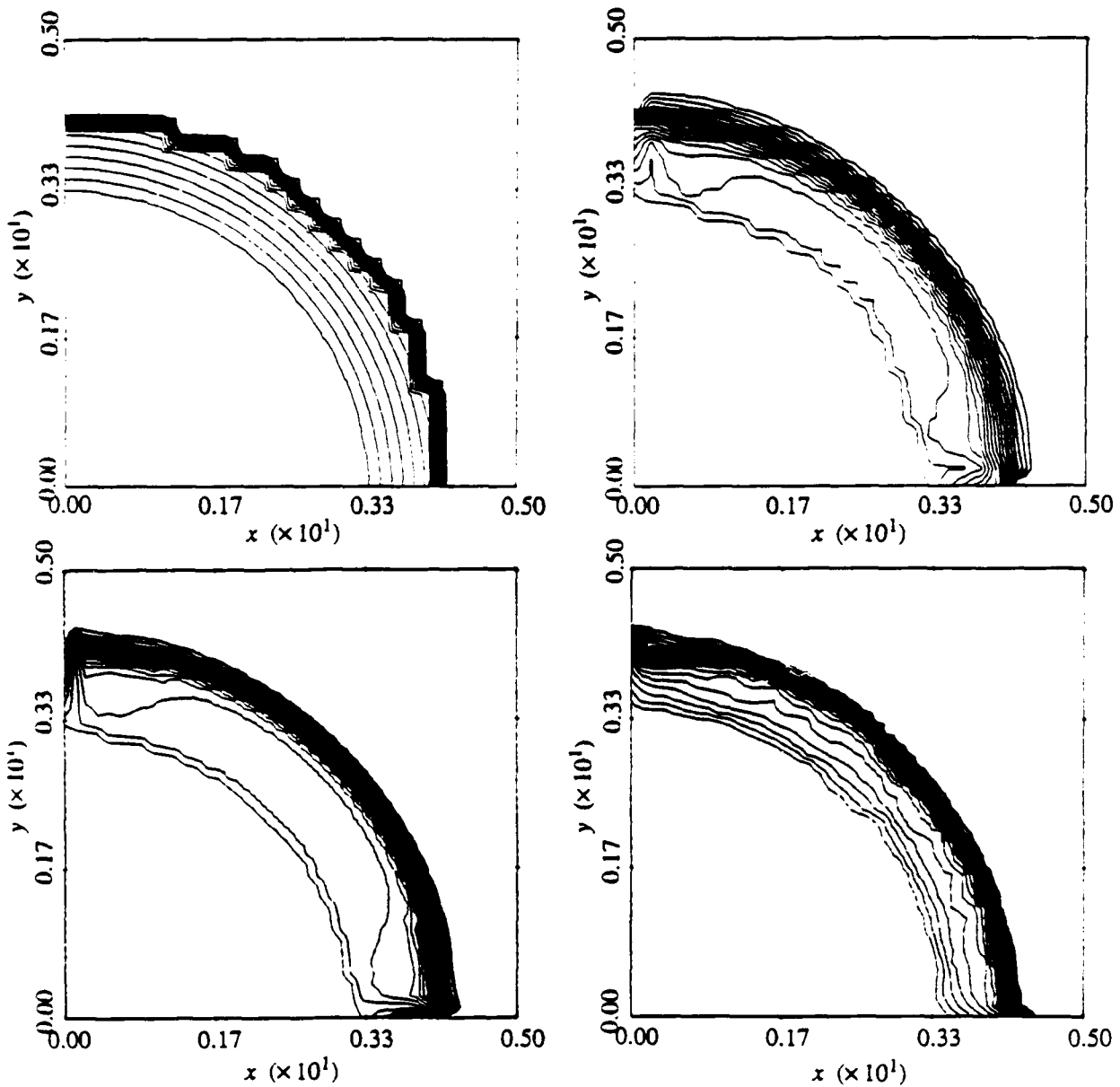


Figure 7. Density contours for Example 2 at $t = 0.0096$ obtained from the exact solution (upper left) and by computed solutions on a uniform stationary mesh (upper right), a uniform stationary base mesh with one level of refinement (lower left), and a moving base mesh with one level of refinement (lower right).

a priori fashion by extrapolating the mesh behavior of the previous two base time steps. As a result, mesh refinement may be inefficient but it never leads to anomalous behavior. On the other hand, incorrect mesh motion can easily mess a local nonuniformity in the solution that evolves suddenly. Such incorrect motion restricts the size of the time steps and diminishes the overall efficiency of the adaptive method. These difficulties can largely be overcome by combining mesh motion with mesh refinement and static mesh redistribution. Further experimentation and analysis are needed in order to determine

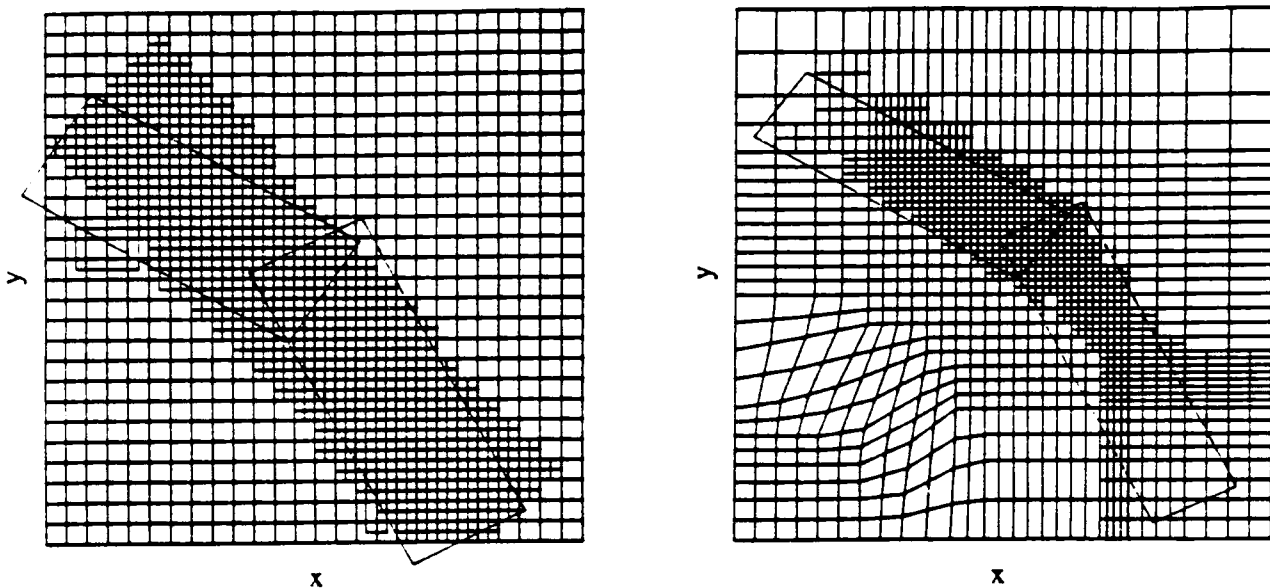


Figure 8. Spatial meshes at $t = 0.0096$ for Example 2 using one level of local mesh refinement on a uniform stationary base mesh (left) and a moving base mesh (right).

optimal combinations of these strategies.

We used the first example to demonstrate that each problem has an optimal initial base mesh size and that it is always computationally efficient to adaptively refine beginning with a less than optimal mesh rather than starting with too fine a mesh. This example also showed that for mesh motion to be effective, a fine base mesh is absolutely necessary. A combination of both the adaptive strategies of mesh motion and refinement produced the best results but at the cost of a significantly higher computational effort. The second example demonstrates that our adaptive mesh procedures extend to two-dimensional problems.

We are currently developing higher-order explicit finite volume methods to replace the second-order MacCormack scheme. The present Richardson's extrapolation-based error indicator is expensive and we are seeking ways of replacing it by using p-refinement techniques. Such methods have been shown to have an excellent cost performance ratio when used in conjunction with finite element methods. We are also working on a modification of our algorithm which allows a variety of geometries. Our adaptive techniques must be able to take advantage of the latest advances in vector and parallel computing hardware. The tree is a highly parallel structure and we are developing solution procedures that exploit this in a variety of shared and distributed memory parallel computing environments; however, it is difficult to parallelize mesh motion because of its global nature. Cells assigned to a particular processor may migrate to the domain of other neighboring processors and cause non-trivial bookkeeping problems. Mesh motion is also difficult to

perform in higher dimensions. We are, therefore, actively considering hp-type techniques in parallel environments.

REFERENCES.

1. Arney, D.C., Biswas, R., and Flaherty, J.E., "Adaptive Mesh Experiments for Hyperbolic Partial Differential Equations," *Trans. Sixth Army Conf. Appl. Math. and Comput.*, (1989), pp. 1051-1074.
2. Arney, D.C., Biswas, R., and Flaherty, J.E., "A Posteriori Error Estimation of Adaptive Finite Difference Schemes for Hyperbolic Systems," *Trans. Fifth Army Conf. Appl. Math. and Comput.*, (1988), pp. 437-458.
3. Arney, D.C., Carofano, G., and Misner, E., "An Adaptive Mesh Method for Solving Blast Problems Using the Euler Equations," *Trans. Sixth Army Conf. Appl. Math. and Comput.*, (1989), pp. 1115-1132.
4. Arney, D.C. and Flaherty, J.E., "An Adaptive Mesh Moving and Local Refinement Method for Time-Dependent Partial Differential Equations," to appear in *Trans. Math. Software*.
5. Arney, D.C. and Flaherty, J.E., "A Two-Dimensional Mesh Moving Technique for Time Dependent Partial Differential Equations," *J. Comput. Phys.*, **67** (1986), pp. 124-144.
6. Arney, D.C. and Flaherty, J.E., "An Adaptive Local Mesh Refinement Method for Time Dependent Partial Differential Equations," *Appl. Num. Math.*, **5** (1989), pp. 257-274.
7. Coyle, J.M., Flaherty, J.E., and Ludwig, R., "On the Stability of Mesh Equidistribution Strategies for Time-Dependent Partial Differential Equations," *J. Comput. Phys.*, **62** (1986), pp. 26-39.
8. Davis, S., "A Simplified TVD Finite Difference Scheme via Artificial Viscosity," *SIAM J. Sci. Stat. Comput.*, **8** (1987), pp. 1-18.
9. Kimura, T. and Tsutahara, M., "Analysis of Compressible Flows around a Uniformly Expanding Circular Cylinder and Sphere," *J. Fluid. Mech.*, **79** (1977), pp. 625-630.
10. MacCormack, R.W., "The Effect of Viscosity in Hypervelocity Impact Cratering," *AIAA Paper 69-354*, (1969).
11. Richardson, L.F., "The Deferred Approach to the Limit, I. Single Lattice," *Trans. Roy. Soc. London*, **226** (1927), pp. 299-349.
12. Sod, G., "A Survey of Several Finite Difference Methods for Systems of Nonlinear Hyperbolic Conservation Laws," *J. Comp. Phys.*, **27** (1978), pp. 1-31.
13. Whitham, G.B., *Linear and Nonlinear Waves*, Wiley-Interscience, New York, 1974.

TECHNICAL REPORT INTERNAL DISTRIBUTION LIST

	<u>NO. OF COPIES</u>
CHIEF, DEVELOPMENT ENGINEERING DIVISION	
ATTN: SMCAR-CCB-DA	1
-DC	1
-DI	1
-DR	1
-DS (SYSTEMS)	1
CHIEF, ENGINEERING SUPPORT DIVISION	
ATTN: SMCAR-CCB-S	1
-SD	1
-SE	1
CHIEF, RESEARCH DIVISION	
ATTN: SMCAR-CCB-R	2
-RA	1
-RE	1
-RM	1
-RP	1
-RT	1
TECHNICAL LIBRARY	5
ATTN: SMCAR-CCB-TL	
TECHNICAL PUBLICATIONS & EDITING SECTION	3
ATTN: SMCAR-CCB-TL	
OPERATIONS DIRECTORATE	1
ATTN: SMCWV-ODP-P	
DIRECTOR, PROCUREMENT DIRECTORATE	1
ATTN: SMCWV-PP	
DIRECTOR, PRODUCT ASSURANCE DIRECTORATE	1
ATTN: SMCWV-QA	

NOTE: PLEASE NOTIFY DIRECTOR, BENET LABORATORIES, ATTN: SMCAR-CCB-TL, OF ANY ADDRESS CHANGES.

TECHNICAL REPORT EXTERNAL DISTRIBUTION LIST

	<u>NO. OF COPIES</u>		<u>NO. OF COPIES</u>
ASST SEC OF THE ARMY RESEARCH AND DEVELOPMENT ATTN: DEPT FOR SCI AND TECH THE PENTAGON WASHINGTON, D.C. 20310-0103	1	COMMANDER ROCK ISLAND ARSENAL ATTN: SMCRI-ENM ROCK ISLAND, IL 61299-5000	1
ADMINISTRATOR DEFENSE TECHNICAL INFO CENTER ATTN: DTIC-FDAC CAMERON STATION ALEXANDRIA, VA 22304-6145	12	DIRECTOR US ARMY INDUSTRIAL BASE ENGR ACTV ATTN: AMXIB-P ROCK ISLAND, IL 61299-7260	1
COMMANDER US ARMY ARDEC ATTN: SMCAR-AEE	1	COMMANDER US ARMY TANK-AUTMV R&D COMMAND ATTN: AMSTA-DDL (TECH LIB) WARREN, MI 48397-5000	1
SMCAR-AES, BLDG. 321	1	COMMANDER US MILITARY ACADEMY	1
SMCAR-AET-O, BLDG. 351N	1	ATTN: DEPARTMENT OF MECHANICS WEST POINT, NY 10996-1792	
SMCAR-CC	1		
SMCAR-CCP-A	1	US ARMY MISSILE COMMAND	
SMCAR-FSA	1	REDSTONE SCIENTIFIC INFO CTR	2
SMCAR-FSM-E	1	ATTN: DOCUMENTS SECT, BLDG. 4484 REDSTONE ARSENAL, AL 35898-5241	
SMCAR-FSS-D, BLDG. 94	1		
SMCAR-IMI-I (STINFO) BLDG. 59	2		
PICATINNY ARSENAL, NJ 07806-5000			
DIRECTOR US ARMY BALLISTIC RESEARCH LABORATORY ATTN: SLCBR-DD-T, BLDG. 305 ABERDEEN PROVING GROUND, MD 21005-5066	1	COMMANDER US ARMY FGN SCIENCE AND TECH CTR ATTN: DRXST-SD 220 7TH STREET, N.E. CHARLOTTESVILLE, VA 22901	1
DIRECTOR US ARMY MATERIEL SYSTEMS ANALYSIS ACTV ATTN: AMXSY-MP ABERDEEN PROVING GROUND, MD 21005-5071	1	COMMANDER US ARMY LABCOM MATERIALS TECHNOLOGY LAB ATTN: SLCMT-IML (TECH LIB) WATERTOWN, MA 02172-0001	2
COMMANDER HQ, AMCCOM ATTN: AMSMC-IMP-L ROCK ISLAND, IL 61299-6000	1		

NOTE: PLEASE NOTIFY COMMANDER, ARMAMENT RESEARCH, DEVELOPMENT, AND ENGINEERING CENTER, US ARMY AMCCOM, ATTN: BENET LABORATORIES, SMCAR-CCB-TL, WATERVLIET, NY 12189-4050, OF ANY ADDRESS CHANGES.

TECHNICAL REPORT EXTERNAL DISTRIBUTION LIST (CONT'D)

	<u>NO. OF COPIES</u>		<u>NO. OF COPIES</u>
COMMANDER US ARMY LABCOM, ISA ATTN: SLCIS-IM-TL 2800 POWDER MILL ROAD ADELPHI, MD 20783-1145	1	COMMANDER AIR FORCE ARMAMENT LABORATORY ATTN: AFATL/MN EGLIN AFB, FL 32542-5434	1
COMMANDER US ARMY RESEARCH OFFICE ATTN: CHIEF, IPO P.O. BOX 12211 RESEARCH TRIANGLE PARK, NC 27709-2211	1	COMMANDER AIR FORCE ARMAMENT LABORATORY ATTN: AFATL/MNF EGLIN AFB, FL 32542-5434	1
DIRECTOR US NAVAL RESEARCH LAB ATTN: MATERIALS SCI & TECH DIVISION CODE 26-27 (DOC LIB) WASHINGTON, D.C. 20375	1 1	MIAC/CINDAS PURDUE UNIVERSITY 2595 YEAGER ROAD WEST LAFAYETTE, IN 47905	1
DIRECTOR US ARMY BALLISTIC RESEARCH LABORATORY ATTN: SLCBR-IB-M (DR. BRUCE BURNS) ABERDEEN PROVING GROUND, MD 21005-5066	1		

NOTE: PLEASE NOTIFY COMMANDER, ARMAMENT RESEARCH, DEVELOPMENT, AND ENGINEERING CENTER, US ARMY AMCCOM, ATTN: BENET LABORATORIES, SMCAR-CCB-TL, WATERVLIET, NY 12189-4050, OF ANY ADDRESS CHANGES.